

Decamethylsilocene – The First Stable Silicon(II) Compound: Synthesis, Structure, and Bonding

Peter Jutzi*^a, Udo Holtmann^a, Dieter Kanne^a, Carl Krüger^b, Richard Blom^c, Rolf Gleiter^d, and Isabella Hyla-Krystin^d

Fakultät für Chemie der Universität Bielefeld^a,
Universitätsstraße, D-4800 Bielefeld, F. R. G.

Max-Planck-Institut für Kohlenforschung^b,
Kaiser-Wilhelm-Platz 1, D-4330 Mülheim-Ruhr, F. R. G.

Department of Chemistry, University of Oslo^c,
Blindern, N-0315 Oslo 3, Norway

Organisch-Chemisches Institut der Universität Heidelberg^d,
Im Neuenheimer Feld 270, D-6900 Heidelberg, F. R. G.

Received March 17, 1989

Key Words: Calculations, MNDO and HF / GED data / PE spectra / Silocene, decamethyl- / Silicon(II) π -complexes

Reaction of dichlorobis(pentamethylcyclopentadienyl)silane with naphthalene-lithium, -sodium, or -potassium leads to elemental silicon and to decamethylsilocene, $(\text{Me}_5\text{C}_5)_2\text{Si}$ (**4**). Compound **4** is formed as the only product in the reduction of dibromobis(pentamethylcyclopentadienyl)silane with anthracene-potassium. **4** is a thermally stable, colorless, air-sensitive π -complex. Its NMR spectra are typical for a group 14 metallocene; the ^{29}Si -NMR signal appears at very high field strength ($\delta = -398$ ppm). CV and MS data of **4** prove the instability of the $(\text{Me}_5\text{C}_5)_2\text{Si}^{\oplus}$ ion, which easily loses a Me_5C_5 radical. X-ray crystallographic studies show the presence of two geometrical isomers, **4a** and **4b**, in the monoclinic unit cell. Isomer **4a** is isotypical with decamethylferrocene, isomer **4b** possesses the expected bent-metallocene-type structure. Space-filling models indicate the interplane angle in **4b** to be of the largest possible value. Due to GED studies, **4** has a bent-metallocene-type structure in the gas phase. The He(I) PE spectrum of **4** is compared with those of the heavier homologues $(\text{Me}_5\text{C}_5)_2\text{Ge}$ (**6**), $(\text{Me}_5\text{C}_5)_2\text{Sn}$ (**7**), and $(\text{Me}_5\text{C}_5)_2\text{Pb}$ (**8**). A strong shift to higher energy of the band assigned to the group 14 element lone pair is observed in going from **8**, **7**, or **6** to **4**. Calculations have been carried out for structural models of the parent silocene, $(\text{H}_5\text{C}_5)_2\text{Si}$, on the basis of the MNDO procedure and of the HF theory (STO-3G and STO-3G* basis sets). The calculated geometrical parameters and orbital energies are compared with those derived from the GED experiment and from the PE spectrum. The bathochromic shift in the electronic absorption spectra going from **4** to **6–8** is explained on the basis of MNDO calculations for the parent metallocenes.

In the organometallic chemistry of the group 14 elements germanium, tin, and lead it is possible to stabilize the oxidation state +2 by π -complex formation¹. In this context, arene, carbollyl, and cyclopentadienyl systems have been shown to be important as ligands to divalent group 14 centers. In π -cyclopentadienyl chemistry, the introduction of the pentamethylcyclopentadienyl ligand has allowed the syn-

Decamethylsilocen – die erste stabile Silicium(II)-Verbindung: Synthese, Struktur und Bindungsverhältnisse

Die Reaktion von Dichlorbis(pentamethylcyclopentadienyl)silan mit Naphthalin-Lithium, -Natrium oder -Kalium führt zu elementarem Silicium und zu Decamethylsilocen (**4**). Bei der Reaktion von Dibrombis(pentamethylcyclopentadienyl)silan mit Anthracen-Kalium wird ausschließlich **4** gebildet. **4** ist ein thermisch stabiler, farblos, luftempfindlicher π -Komplex. Seine NMR-Spektren sind typisch für Metallocene der Gruppe 14; das ^{29}Si -NMR-Signal erscheint bei sehr hohen Feldstärken ($\delta = -398$ ppm). CV- und MS-Daten von **4** belegen die Instabilität des $(\text{Me}_5\text{C}_5)_2\text{Si}^{\oplus}$ -Ions, das leicht ein Me_5C_5 -Radikal verliert. Nach Röntgenstrukturuntersuchungen liegen zwei geometrische Isomere, **4a** und **4b**, in der monoklinen Elementarzelle vor. Isomer **4a** ist isotyp mit Decamethylferrocen, Isomer **4b** besitzt die erwartete Struktur eines gewinkelten Metallocens. Nach Modellbetrachtungen liegt in **4b** der größtmögliche Interplanar-Winkel vor. GED-Studien belegen für **4** eine gewinkelte Metallocen-Struktur in der Gasphase. Das He(I)-PE-Spektrum von **4** wird mit denjenigen der schwereren Homologen $(\text{Me}_5\text{C}_5)_2\text{Ge}$ (**6**), $(\text{Me}_5\text{C}_5)_2\text{Sn}$ (**7**) und $(\text{Me}_5\text{C}_5)_2\text{Pb}$ (**8**) verglichen. Für die Bande, die dem freien Elektronenpaar des Gruppe-14-Elements zugeordnet wird, ist beim Übergang von **8**, **7** oder **6** zu **4** eine starke Verschiebung zu höherer Energie zu beobachten. Strukturmodelle der Stammverbindung $(\text{H}_5\text{C}_5)_2\text{Si}$ sind auf der Basis des MNDO-Konzepts und der HF-Theorie (STO-3G- und STO-3G*-Basissätze) berechnet worden. Die berechneten geometrischen Parameter und Orbital-Energien werden mit denjenigen aus dem GED-Experiment und dem PE-Spektrum verglichen. Die bathochrome Verschiebung in den Elektronenanregungsspektren beim Übergang von **4** zu **6–8** wird unter Zugrundelegung von MNDO-Rechnungen für die H-substituierten Metallocene erklärt.

thesis of many thermally stable, but still highly reactive complexes. In this class of compounds, the decamethylmetallocenes of germanium, tin, and lead play a dominant role.

So far, no inorganic or organometallic species with divalent silicon has been shown to be stable under normal conditions^{2,3}. To change this situation, π -complexation seemed to us to be an interesting tool. Here we describe

synthesis and characterization of decamethylsilocene (**4**), the first stable compound with silicon in the oxidation state +2.

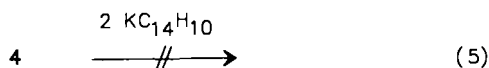
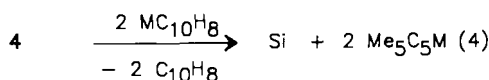
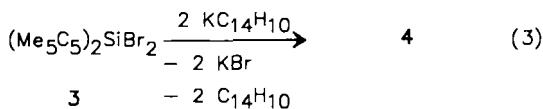
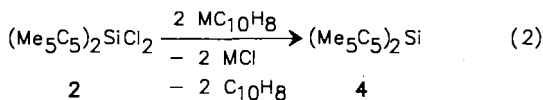
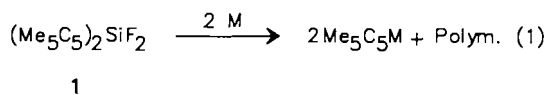
Synthesis of Decamethylsilocene (**4**)

Due to the fact that no substrates with divalent silicon are available, it was necessary to start with compounds containing tetravalent silicon and to try the synthesis of **4** by a reductive process. The bis(η^1 -pentamethylcyclopentadienyl)-silicon dihalides **1**–**3** seemed to be suitable compounds for this purpose. Their synthesis and structure have been described only recently⁴⁾.

In previous experiments we have already shown that the reductive process offers an alternative route to the decamethylmetallocenes of germanium and tin⁵⁾. Thus, reaction of the bis(η^1 -pentamethylcyclopentadienyl)element dichlorides and -bromides with reducing agents (naphthalene-alkali metal compounds, cyclooctatetraene-dipotassium) leads to the desired metallocenes. Special reaction conditions have to be chosen to avoid further reduction to the corresponding group 14 metal.

The difluorobis(pentamethylcyclopentadienyl)silane (**1**) reacts with alkali metals or naphthalene-alkali metal compounds to give mainly the corresponding alkali metal pentamethylcyclopentadienides and a SiF-containing polymer (eq. 1), thus indicating that in **1** the pentamethylcyclopentadienyl ligand⁶⁾ is the better leaving group than the fluoro ligand.

In the reaction of dichlorobis(pentamethylcyclopentadienyl)silane (**2**) with naphthalene-lithium, -sodium, and -potassium, a grey-black suspension is formed. After filtration, elemental silicon is obtained from the residue. From the colorless solution, decamethylsilocene (**4**) can be isolated after removal of the solvent and fractional sublimation of the remaining material (eq. 2)⁷⁾. Starting from **2**, the highest yield of **4** is obtained by performing the reactions at



M=Li,Na,K

–50°C in dimethoxyethane as the solvent and using a 50% excess of the sodium compound (see experimental part).

The undesired formation of elemental silicon is avoided by using the dibromosilane **3** as the substrate and anthracene-potassium as the reducing agent (eq. 3).

Recrystallization from *n*-pentane gives colorless crystals of **4**, which are soluble in all common aprotic organic solvents. According to cryoscopic molecular-weight determinations, compound **4** is monomeric in benzene solution. It is stable in the air for short times of exposure, but sensitive against hydrolysis; it melts at 171°C without decomposition.

From the results of the reactions described in eq. 2 and 3, it can be assumed that **4** is further reduced by naphthalene-alkali metal compounds, but not by anthracene-potassium. This assumption was proved in separate experiments which demonstrate the well-known differences in the reactivity of radical anions and dianions of aromatic species⁸⁾. Thus, decamethylsilocene (**4**) reacts with naphthalene-sodium quantitatively to elemental silicon and to sodium pentamethylcyclopentadienide (eq. 4), whereas it does not react with anthracene-potassium (eq. 5).

NMR Data of **4**

On the basis of observations in the ¹H- and ¹³C-NMR spectra of the metallocenes of germanium, tin, and lead, only averaged signals for all ring carbons and for all methyl groups are expected in the NMR spectra of **4**. Indeed, the ¹H-NMR spectrum of **4** reveals a very sharp singlet at $\delta = 1.89$; in the ¹³C-NMR spectrum, the signal for the ring carbons appears at $\delta = 119.1$ and that for the methyl carbons at $\delta = 10.0$. These observations are in accord with a more or less symmetrical π -structure and quickly rotating pentamethylcyclopentadienyl rings. Principally, they do not exclude a highly fluxional species with σ -bonded cyclopentadienyl rings. The latter structure is excluded from the ²⁹Si-NMR spectrum of **4**, where a resonance at very high field strength ($\delta = -398$) is observed. In comparison with the high-field chemical shift in the ¹¹⁹Sn-NMR spectrum of decamethylstannocene^{5,9)} or in the ²⁰⁷Pb-NMR spectrum of decamethylplumbocene⁹⁾, this proves the assumed π -structure for **4**. The chemical shift in the ²⁹Si-NMR spectrum of **4** has the highest value so far observed for an organosilicon compound.

CV and MS Data of **4**

CV measurements in dichloromethane as the solvent and NBu₄⁺BF₄⁻ as supporting electrolyte show that **4** cannot be reduced in the region available (up to –1.7 V versus SCE). This observation is consistent with the chemical behavior of **4** in reduction processes, as described in eq. 4 and 5. An irreversible oxidation process takes place at +0.4 V versus SCE. Presumably the radical cation of **4** is unstable due to the easy formation of the comparatively very stable pentamethylcyclopentadienyl radical¹⁰⁾. The fate of the remaining Me₅C₅Si⁺ ion is uncertain. Further irreversible oxidation processes are observed in the region from +0.8 to +1.5 V versus SCE. Comparable results have been obtained from

the CV data of decamethylgermanocene (**6**) and -stannocene (**7**)¹¹.

The mass spectrum of **4** has been performed by electron impact (EI, 70 eV) and by chemical ionization (CI, isobutane). Interestingly, the molecular ion is not observed in both types of measurements. The fragment with the highest mass ($m/z = 163$) corresponds to the $\text{Me}_5\text{C}_5\text{Si}^{\oplus}$ ion. Further fragmentations of this cation can be detected in the EI spectrum; in the CI spectrum, where the probability of fragmentation

is less, $\text{Me}_5\text{C}_5\text{Si}^{\oplus}$ is the only detectable species. These observations complete those of the cyclovoltammetric studies. It is demonstrated by the CV and MS data, that a $(\text{Me}_5\text{C}_5)_2\text{Si}^{\oplus}$ radical ion is rather unstable in solution and in the gas phase, and easily loses a Me_5C_5 radical.

Crystal Structure of **4**

The results of an X-ray crystal structure analysis of **4** are presented in Figures 1 and 2 and in Tables 1–3.

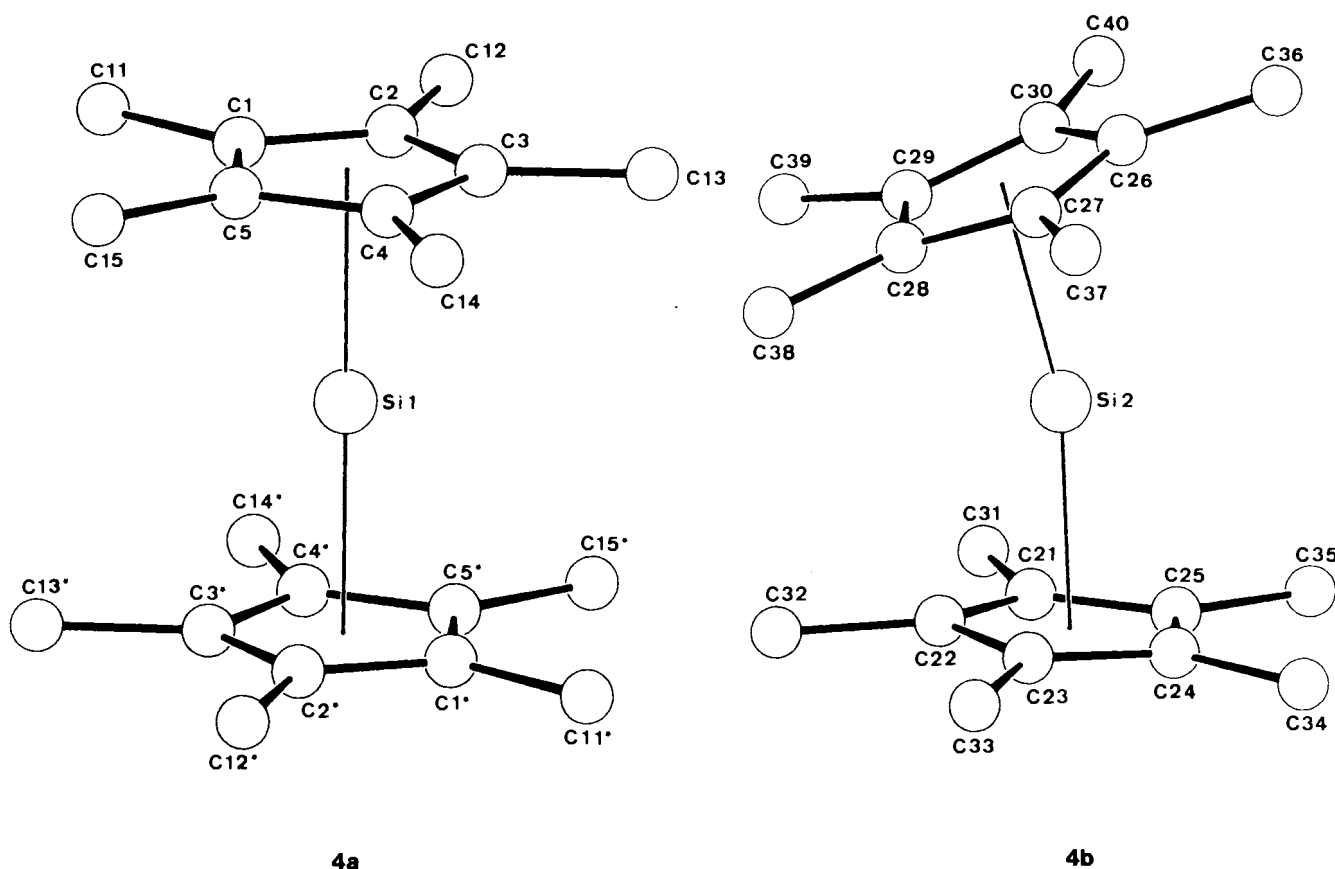


Figure 1. Crystal structure of **4a** and **4b**

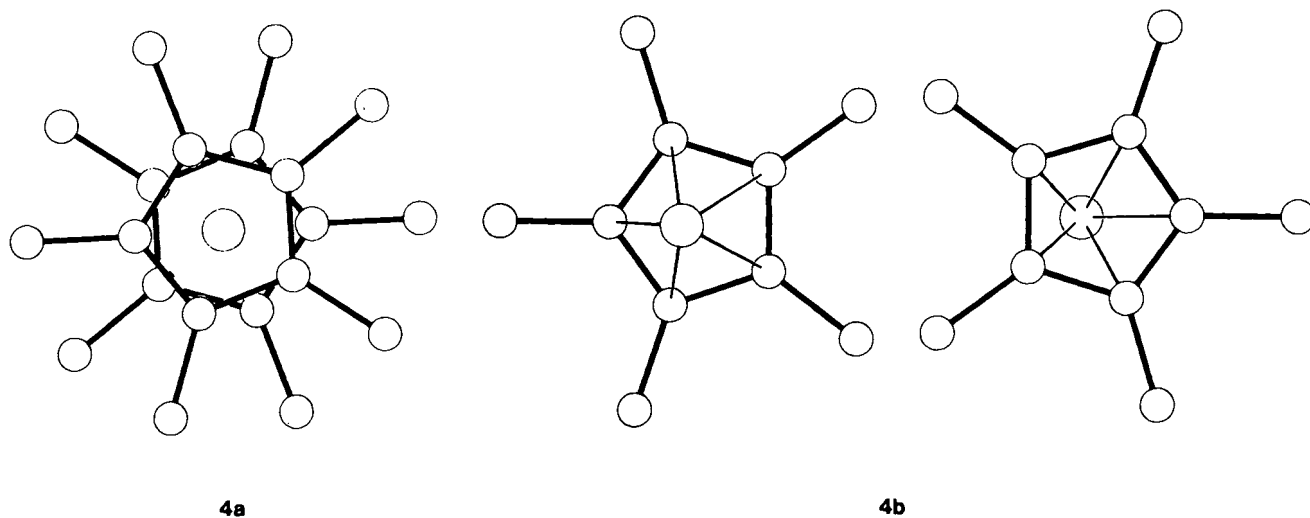


Figure 2. Projection of the silicon atom parallel to the pentamethylcyclopentadienyl ring normal in **4a** and **4b**

Table 1. X-ray diffraction data for **4**^{a)}

Formula: C₂₀H₃₀Si; mol. mass: 298.5; crystal size: 0.25 × 0.61 × 0.54 mm; colourless; *a* = 31.969(5), *b* = 8.525(1), *c* = 23.212(3) Å; β = 108.75(1)°; *V* = 5990 Å³; *d*_{calcd.} = 0.99 g cm⁻³; μ = 1.08 cm⁻¹; absorption correction: empirically; monoclinic; space group *C2/c*; *Z* = 12; *F*(000) = 1968; radiation: Mo-*K*_α; λ = 0.71069 Å; (sin θ/λ)_{max} = 0.65; diffractometer: Nonius CAD4; scan technique: ω/2θ; temperature: 293 K; measured reflections: 7598 (±*h* + *k* + *l*); unique reflections: 6746; observed reflections: 2611 [*I* > 2σ(*I*)]; solution: heavy-atom method; H-atoms: calculated; refined parameters: 286; *R* = 0.088, *R*_w = 0.096 [*w* = 1/σ²(*F*_o)]; final residual electron density: 0.24 e Å⁻³.

^{a)} Further details of the crystal structure investigation are available on request from the Fachinformationszentrum Energie, Physik, Mathematik GmbH, D-7514 Eggenstein-Leopoldshafen 2, on quoting the depository number CSD-51619, the names of the authors, and the journal citation.

Table 2. Bond distances [Å] and bond angles [°] of **4a** and **4b**^{a)}

Si1 - D1	2.114(2)	D1* - Si1	180.0
Si1 - C1	2.434(1)	C11 - C1	125.1(1)
Si1 - C2	2.409(1)	C11 - C1 - C2	126.9(1)
Si1 - C3	2.414(1)	C5 - C1 - C2	108.0(1)
Si1 - C4	2.420(1)	C12 - C2 - C3	126.1(1)
Si1 - C5	2.442(1)	C12 - C2 - C1	125.4(1)
C1 - C2	1.401(1)	C3 - C2 - C1	108.5(1)
C1 - C5	1.393(1)	C13 - C3 - C4	125.7(1)
C1 - C11	1.493(1)	C13 - C3 - C2	125.9(1)
C2 - C3	1.370(1)	C4 - C3 - C2	108.4(1)
C2 - C12	1.510(1)	C14 - C4 - C5	125.7(1)
C3 - C4	1.400(1)	C14 - C4 - C3	126.6(1)
C3 - C13	1.508(1)	C5 - C4 - C3	107.6(1)
C4 - C5	1.408(1)	C15 - C5 - C4	125.4(1)
C4 - C14	1.508(1)	C15 - C5 - C1	127.2(1)
C5 - C15	1.496(1)	C4 - C5 - C1	107.4(1)
Si2 - D2	2.120(2)	D3 - Si2	167.4(7)
Si2 - D3	2.122(2)	C31 - C21 - C25	124.7(7)
Si2 - C21	2.417(7)	C31 - C21 - C22	126.2(6)
Si2 - C22	2.323(7)	C25 - C21 - C22	109.2(6)
Si2 - C23	2.375(7)	C32 - C22 - C23	126.5(6)
Si2 - C24	2.502(7)	C32 - C22 - C21	125.4(6)
Si2 - C25	2.526(7)	C23 - C22 - C21	107.4(6)
Si2 - C26	2.541(7)	C33 - C23 - C24	126.9(6)
Si2 - C27	2.445(8)	C33 - C23 - C22	125.5(6)
Si2 - C28	2.324(8)	C24 - C23 - C22	107.5(6)
Si2 - C29	2.347(7)	C34 - C24 - C25	127.3(7)
Si2 - C30	2.489(7)	C34 - C24 - C23	123.9(7)
C21 - C22	1.39 (1)	C25 - C24 - C23	108.7(6)
C21 - C25	1.40 (1)	C35 - C25 - C24	125.3(7)
C21 - C31	1.51 (1)	C35 - C25 - C21	127.5(7)
C22 - C23	1.397(9)	C24 - C25 - C21	107.2(6)
C22 - C32	1.50 (1)	C36 - C26 - C30	125.7(7)
C23 - C24	1.41 (1)	C36 - C26 - C27	125.6(7)
C23 - C33	1.50 (1)	C30 - C26 - C27	108.7(7)
C24 - C25	1.38 (1)	C37 - C27 - C28	124.4(7)
C24 - C34	1.51 (1)	C37 - C27 - C26	127.0(7)
C25 - C35	1.50 (1)	C28 - C27 - C26	108.7(7)
C26 - C27	1.37 (1)	C38 - C28 - C29	126.0(8)
C26 - C30	1.37 (1)	C38 - C28 - C27	126.1(8)
C26 - C36	1.50 (1)	C29 - C28 - C27	107.4(7)
C27 - C28	1.40 (1)	C39 - C29 - C30	127.8(8)
C27 - C37	1.50 (1)	C39 - C29 - C28	125.7(8)
C28 - C29	1.42 (1)	C30 - C29 - C28	106.2(7)
C28 - C38	1.52 (1)	C40 - C30 - C29	124.6(7)
C29 - C30	1.41 (1)	C40 - C30 - C26	126.3(7)
C29 - C39	1.48 (1)	C29 - C30 - C26	109.0(7)
C30 - C40	1.49 (1)		

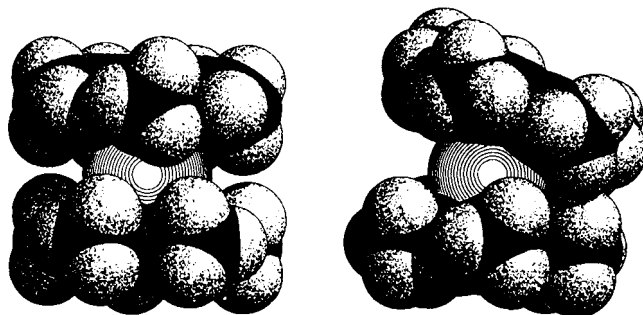
^{a)} D1 is the centroid of the Me₅C₅ ring C1 to C5, D2 is the centroid of the Me₅C₅ ring C21 to C25, D3 is the centroid of the Me₅C₅ ring C26 to C30.

Surprisingly, two geometrical isomers, **4a** and **4b**, are present in the unit cell in the ratio 1:2⁷⁾. Isomer **4a** is isotypical with decamethylferrocene, i.e. the silicon atom occupies a center of inversion, and two pentamethylcyclopentadienyl rings are parallel and staggered. The lone pair at silicon is not stereochemically active. Isomer **4b** is of a bent-metalocene-type structure, typical of the heavier homo-

Table 3. Atomic fractional coordinates and equivalent isotropic thermal parameters [Å²] with standard deviations in parentheses
$$U_{eq} = 1/3 \sum_i \sum_j U_{ij} a_i^* a_j^* \bar{a}_i \cdot \bar{a}_j$$

Atom	x	y	z	U _{eq}
Si(1)	0.0000	0.5000	0.0000	0.075
Si(2)	0.6660(1)	0.3836(2)	0.3265(1)	0.064
C(1)	-0.0723(2)	0.5220(8)	0.0130(3)	0.065
C(2)	-0.0564(2)	0.6741(8)	0.0108(3)	0.066
C(3)	-0.0201(2)	0.6967(7)	0.0612(3)	0.062
C(4)	-0.0121(2)	0.5583(8)	0.0954(3)	0.062
C(5)	-0.0451(2)	0.4495(7)	0.0653(3)	0.061
C(11)	-0.1117(2)	0.448(1)	-0.0321(4)	0.116
C(12)	-0.0763(3)	0.793(1)	-0.0386(4)	0.126
C(13)	0.0074(3)	0.8438(8)	0.0763(3)	0.102
C(14)	0.0239(2)	0.5310(9)	0.1548(3)	0.113
C(15)	-0.0496(3)	0.2875(8)	0.0872(3)	0.102
C(21)	0.5869(2)	0.3528(9)	0.2822(3)	0.068
C(22)	0.6082(2)	0.2093(8)	0.2859(3)	0.059
C(23)	0.6314(2)	0.2122(8)	0.2443(3)	0.067
C(24)	0.6241(2)	0.3602(9)	0.2154(3)	0.073
C(25)	0.5972(2)	0.4470(8)	0.2391(3)	0.070
C(26)	0.7364(2)	0.5142(8)	0.3929(3)	0.073
C(27)	0.7450(2)	0.362(1)	0.3813(3)	0.081
C(28)	0.7201(3)	0.2622(8)	0.4056(3)	0.080
C(29)	0.6953(3)	0.358(1)	0.4325(3)	0.086
C(30)	0.7066(2)	0.5140(9)	0.4244(3)	0.074
C(31)	0.5578(3)	0.403(1)	0.3188(4)	0.118
C(32)	0.6010(2)	0.0692(8)	0.3207(3)	0.090
C(33)	0.6566(3)	0.0774(9)	0.2302(3)	0.101
C(34)	0.6441(3)	0.4107(9)	0.1679(3)	0.115
C(35)	0.5825(3)	0.6121(9)	0.2215(4)	0.121
C(36)	0.7549(3)	0.6575(9)	0.3722(4)	0.112
C(37)	0.7755(3)	0.307(1)	0.3483(4)	0.136
C(38)	0.7236(3)	0.0847(9)	0.4095(4)	0.146
C(39)	0.6669(3)	0.301(1)	0.4676(3)	0.151
C(40)	0.6873(3)	0.655(1)	0.4444(4)	0.125

logues of **4**, with an interplane angle of 25° and with pentamethylcyclopentadienyl rings asymmetrically bonded in a staggered conformation. In this isomer the lone pair at silicon can be stereochemically active. The Si-C separations are equidistant in molecule **4a** [average value 2.42(1) Å], but different in molecule **4b** [ranging from 2.323(7) Å (C22) to 2.541(7) Å (C26)]. The distance between the silicon atom and the cyclopentadienyl ring centroids is 2.11 Å in **4a** and 2.12 Å in **4b**. In Figure 2, a projection of the silicon atom parallel to the cyclopentadienyl ring normal in **4a** and **4b** is portrayed, clearly showing the ring slippage to an η²/η³-arrangement in **4b**. The lower hapticity of the cyclopentadienyl rings in **4b** is also reflected in the different C-C bond lengths and in the bending of the methyl ligands out of the ring plane. This bending is strongest at the methyl ligands at those ring C atoms which have the shortest C-Si distance (7° at C22, 6° at C28). In molecule **4a**, all methyl groups are approximately (0.03 - 1°) within the planes of the



4a **4b**
Figure 3. Space-filling models for **4a** and **4b**

cyclopentadienyl rings, which are planar within given error limits. Space-filling models clearly indicate the interplanar angle in **4b** to be of the largest possible value: A further bending of the pentamethylcyclopentadienyl ring is not possible due to nonbonding repulsive interactions between the methyl groups on the ring systems (see Figure 3).

Gas-Phase Structure of **4**

The surprising solid-state structure prompted us to investigate also the gas-phase structure of **4** on the basis of its GED patterns. Four main molecular models on the basis of the parent compound $(H_5C_5)_2Si$ (**5**) have been tried out to solve the structure of **4** (see Scheme 1):

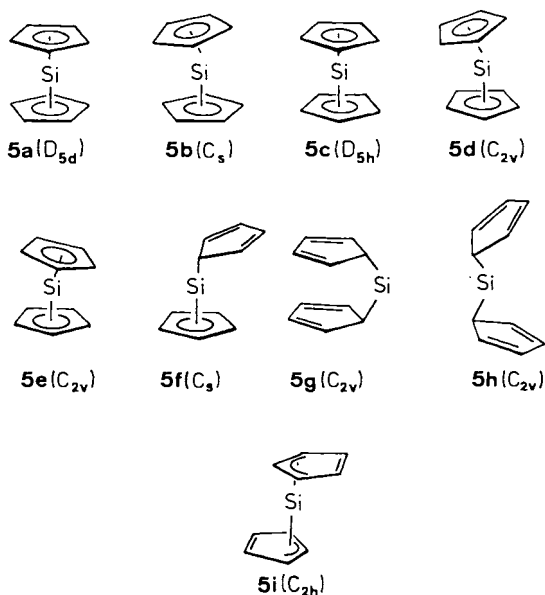
I **5a**–**5e** are structures of minimum D_{5d} , C_s , D_{5h} and C_{2v} symmetry with two η^5 -bonded cyclopentadienyl rings. Structures **5a** and **5c** on the one hand and **5b**, **5d**, **5e** on the other hand are rotamers. **5d** and **5e** can be derived from **5c** by bending both rings, **5b** can be derived from **5a** analogously.

II **5f** is a structure of C_s symmetry with one cyclopentadienyl ring bonded η^1 (or σ) and the other bonded η^5 .

III **5g** and **5h** are rotamers with both rings bonded η^1 .

IV **5i** is a structure of C_{2h} symmetry with two η^3 -bonded cyclopentadienyl rings.

Scheme 1. Model structures for $(H_5C_5)_2Si$



Models II to IV could not be brought into agreement with the experimental data. On the other hand a model with two cyclopentadienyl rings nonparallel and essentially η^5 -bonded to the Si atom could easily be fitted to the experimental data: **5b** with two cyclopentadienyl rings in a staggered conformation and an overall C_s symmetry was the best model (see Figure 4). This model gave a slightly better fit of the theoretical molecular intensity data to the experimental ones than models of C_{2v} symmetry with the cyclopentadienyl ligands in an eclipsed conformation (**5d** and **5e**).

A number of assumptions had to be made in order to decrease the number of independent parameters needed to describe the structure of **4** on the basis of model **5b**. Each CCH_3 fragment has local C_{3v} symmetry and each pentamethylcyclopentadienyl ring has C_{5v} symmetry with the methyl groups fixed in positions with two hydrogens pointing towards the Si atom. The molecular geometry can then be described by eight independent parameters: the distance, d , from the Si atom to the center of the cyclopentadienyl ring; three bond distances C1–C2, C1–C11, and C–H; the angles between the ring plane C_5 and the C–C (Me) bonds, $\angle C_5$, C–C (Me); the CCH valence angle; two parameters that describe the noncoplanarity of the cyclopentadienyl rings. In addition to these eight independent parameters, the distance C11...C13 was refined as an independent parameter because of the large unknown shrinkage of this distance, and 12 root-mean-square amplitudes of vibration (l values) were refined as indicated in Table 4. The nonrefined l values were taken from GED investigations of similar molecules¹².

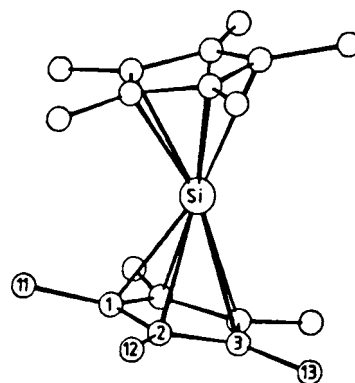


Figure 4. The best molecular model of $(Me_5C_5)_2Si$ in the gas phase; all the H atoms are omitted for clarity; the numbering of the C atoms is shown

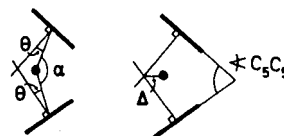


Figure 5. Definition of the bend angle, α , the tilt angle, Θ , the angle between the ring planes, $\angle C_5C_5$, and the distance between the Si atom and the intersection of the C_5 axis of the cyclopentadienyl rings, Δ

Two different choices of parameters were used to describe the noncoplanarity of the cyclopentadienyl rings (see Figure 5): one scheme uses a bend angle, α , and a tilt angle, Θ , as independent parameters, where Θ is defined as positive as shown in Figure 5. This choice is called Scheme A. Scheme B uses the angle between the two ring planes, $\angle C_5C_5$, and a parameter, Δ , that describes the displacement of the Si atom in the C_5 plane away from the intersection of the two C_5 axes of the cyclopentadienyl rings as independent parameters. Δ is defined as positive as drawn in Figure 5. As can be seen in Table 5, the correlation between the main independent parameters was somewhat smaller for Scheme B, which leads to a somewhat better convergence in the least-square analysis

of the structural parameters. The parameters obtained with the two different schemes were of course equal within one standard deviation.

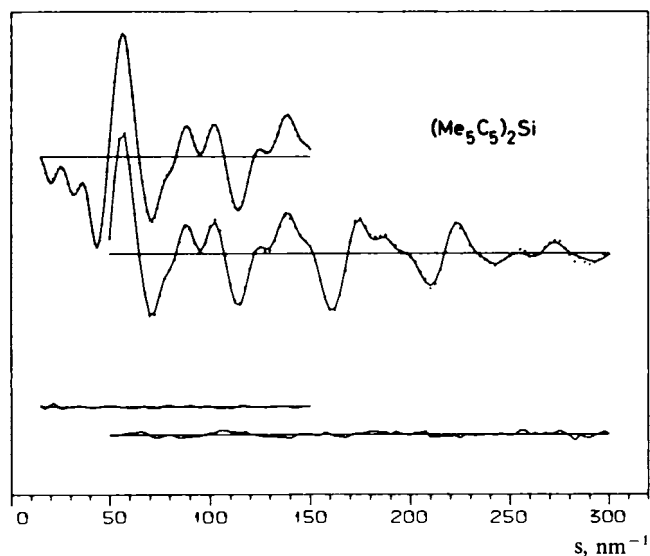


Figure 6. Theoretical molecular intensity curves with experimental points for $(\text{Me}_5\text{C}_5)_2\text{Si}$; the difference between experimental and theoretical curves for the best model are drawn in the lower part of the figure

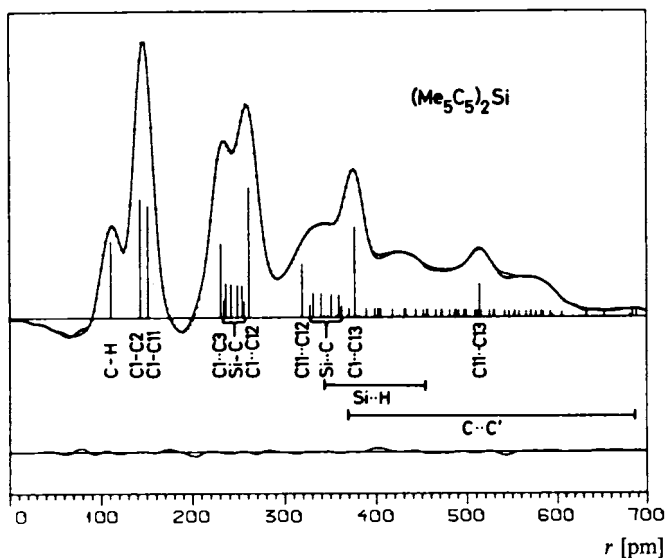


Figure 7. Experimental (points) and theoretical (full line) RD curve for $(\text{Me}_5\text{C}_5)_2\text{Si}$; the most important distances are indicated by bars of height approximately proportional to the area under the corresponding peak; $\text{C}\cdots\text{C}'$ denotes all the carbon-carbon distances from one pentamethylcyclopentadienyl ring to the other; the difference between the experimental and theoretical curves for the best model is drawn in the lower part of the figure; artificial damping constant, k , is 0.02 \AA^2

The theoretical molecular intensity curves with experimental points and difference curves are shown in Figure 6, and the corresponding radial distribution curve is shown in Figure 7. The geometrical parameters and root-mean-square amplitudes of vibration (l values) for the best model are listed

Table 4. The geometrical parameters and root-mean-square amplitudes of vibration (l values) for $(\text{Me}_5\text{C}_5)_2\text{Si}$ in the gas phase; the estimated errors in parentheses are three times the least-squares standard deviations

distances [\AA]	r_a	l
$d^a)$	2.129(12)	—
$r(\text{Si}-\text{C})$ (range)	2.34–2.55	0.132(24)
$r(\text{C1}-\text{C2})$	1.512(4)	0.048(6) ^{e)}
$r(\text{C1}-\text{C11})$	1.512(4)	0.053(6) ^{e)}
$r(\text{C}-\text{H})$	1.105(4)	0.083(4)
$r[\text{Si}\cdots\text{C}(\text{Me})]$ (range)	3.28–3.61	0.161(35)
$r(\text{Si}\cdots\text{H})$ (long)	4.23–4.52	0.200 ^{h)}
$r(\text{Si}\cdots\text{H})$ (short)	3.44–3.79	0.370 ^{h)}
$r(\text{C1}\cdots\text{C3})$	2.30	0.058(5)
$r(\text{C1}\cdots\text{C12})$	2.61	0.079(4)
$r(\text{C1}\cdots\text{C13})$	3.76	0.079(5)
$r(\text{C11}\cdots\text{C12})$	3.19	0.155(24)
$r(\text{C11}\cdots\text{C13})$	5.132(12)	0.088(14)
$r[\text{C}(\text{Cp})\cdots\text{C}(\text{Cp}')]$ (range)	3.88–4.90	0.16–0.19(3)
$r[\text{C}(\text{Cp})\cdots\text{C}(\text{Me}')]$ (range)	3.97–5.94	0.39–0.41(5)
$r[\text{C}(\text{Me})\cdots\text{C}(\text{Me}')]$ (range)	3.69–6.88	0.18–0.20(6)
$\Delta^b)$	0.021(11)	—
angles [$^\circ$]		
$\alpha^c)$	169.6(41)	—
$\Theta^c)$	5.9(20)	—
$\chi \text{ C}_5\text{C}_5^d)$	22.3(12)	—
$\chi \text{ C}_5, \text{C}-\text{C}(\text{Me})^d)$	–0.1(12)	—
$\chi \text{ CCH}$	112.5(10)	—

^{a)} The distance from the Si atom to the ring centers. — ^{b)} The distance from the intersection of the C_5 axis of the two cyclopentadienyl rings. — ^{c)} See Figure 5 for explanation. — ^{d)} This angle is defined as positive if the methyl groups are bent towards the silicon atom. — ^{e)} These two l values were refined with the same shift throughout the least-squares refinements. — ^{h)} Fixed values.

Table 5. The correlation between the main parameters ($\times 100$) for the two different choices of independent parameters as described in the text; Scheme A: The correlation when the bent angle, α , and the tilt angle, Θ , were chosen as independent parameters; Scheme B: The correlation when $\chi \text{ C}_5\text{C}_5$ and the displacement of the Si atom away from the intersection of the C_5 axis of the two cyclopentadienyl rings, Δ , have been used as independent parameters, σ_{ls} is the standard deviation from least squares

Scheme A

	σ_{ls}	d	α	Θ	$l(\text{Si}-\text{C})$	$l(\text{Si}\cdots\text{C})$
d	0.33	—	—	—	—	—
α	1.37	–25	—	—	—	—
Θ	0.67	–28	96	—	—	—
$l(\text{Si}-\text{C})$	0.70	14	–83	–87	—	—
$l(\text{Si}\cdots\text{C})$	1.43	20	–92	–92	78	—

Scheme B

	σ_{ls}	d	Δ	$\chi \text{ C}_5\text{C}_5$	$l(\text{Si}-\text{C})$	$l(\text{Si}\cdots\text{C})$
d	0.41	—	—	—	—	—
Δ	3.44	60	—	—	—	—
$\chi \text{ C}_5\text{C}_5$	0.40	19	9	—	—	—
$l(\text{Si}-\text{C})$	0.79	–59	–90	–10	—	—
$l(\text{Si}\cdots\text{C})$	1.74	–59	–95	2	83	—

Table 6. Main structural parameters of $(\text{Me}_5\text{C}_5)_2\text{M}$ compounds where M is a group 14 element

Method ^{a)}	$d^{b)}$ [Å]	$r(\text{M}-\text{C})^{c)}$ [Å]	$\delta^{d)}$ [Å]	$\angle \text{C}_5\text{C}_5$ [°]	Ref.
$(\text{Me}_5\text{C}_5)_2\text{Si}$ 4a	X	2.11	2.42(1)	0	this work
$(\text{Me}_5\text{C}_5)_2\text{Si}$ 4b	X	2.12	2.42(6)	0.023	this work
$(\text{Me}_5\text{C}_5)_2\text{Si}$ 4	GED	2.129(12)	2.45(2)	0.021	this work
$(\text{Me}_5\text{C}_5)_2\text{Ge}$ 6	GED	2.21(3)	2.52(3)	0.015	14)
$(\text{Me}_5\text{C}_5)_2\text{Sn}$ 7	X	2.39	2.68	0.023	26)
$(\text{Me}_5\text{C}_5)_2\text{Pb}$ 8	X	2.48	2.79	0.029	27)

^{a)} X = X-ray crystallography, GED = gas-phase electron diffraction. – ^{b)} The distance from the central atom to the ring centroid. – ^{c)} Mean distances. – ^{d)} Mean values of the distances from the center of mass of each C_5 ring to the projection of the group 14 element into the ring plane.

in Table 4. The best molecular model of $(\text{Me}_5\text{C}_5)_2\text{Si}$ is shown in Figure 4.

In the gas phase the angle between the C_5 ring planes, $\angle \text{C}_5\text{C}_5$, has been found to be $22.3(12)^\circ$. It must be emphasized that the gas-phase structure is the *thermal average* structure that has not been corrected for ring-Si-ring bending vibrations or ring tilt vibrations (shrinkage effects). The bend and tilt observed for $(\text{Me}_5\text{C}_5)_2\text{Si}$ in the gas phase may therefore be an effect of these large amplitude motions, and from the gas-phase electron diffraction data alone we cannot conclude that the *equilibrium* molecular structure is not the ferrocene like structure with parallel Me_5C_5 rings. This problem has been discussed in ref.¹²⁾ On the other hand the molecular model **5f** with one η^1 - and one η^5 -bonded Me_5C_5 ring, model **5i** with two η^3 -bonded Me_5C_5 rings, or models **5g, h** with two η^1 -bonded Me_5C_5 rings can be ruled out on the basis of the electron diffraction data.

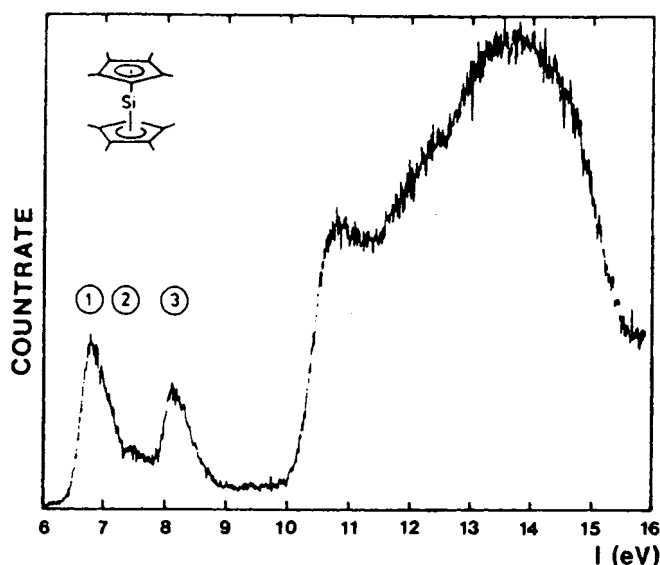
Since we were able to refine the average displacement of the Si atom away from the intersection of the C_5 axes of the cyclopentadienyl rings, we also made some new refinements on old data for the Ge analogue¹³⁾. In the earlier paper on the gas-phase structure of $(\text{Me}_5\text{C}_5)_2\text{Ge}$ each $(\text{Me}_5\text{C}_5)\text{Ge}$ fragment was assumed to be of C_{5v} symmetry¹⁴⁾. In order to check this assumption we used Scheme B as described above. The new refinements did not lead to a significantly better fit of the theoretical molecular intensity curve to the experimental ones, and only a nonsignificant value of Δ of $0.016(19)\text{Å}$ was obtained. Previously, a parameter δ has been used to describe a somewhat distorted η^5 -bonded cyclopentadienyl ring. δ has then been defined as the distance from the center of mass of the C_5 ring to the projection of the central element into the ring plane. The connection between Δ and δ is straightforward, and we have listed δ and the other main structural parameters for the $(\text{Me}_5\text{C}_5)_2\text{M}$ compounds where M is a group 14 element in Table 6.

PES Data of **4** and Calculations for $(\text{H}_5\text{C}_5)_2\text{Si}$ (**5**)

To get further information of the bonding in silicocene, we have recorded the He(I) photoelectron (PE) spectrum of **4** and carried out model calculations on the structural models **5a**–**5i** (see Scheme 1) of the parent compound $(\text{H}_5\text{C}_5)_2\text{Si}$. For the calculations we used the MNDO procedure¹⁵⁾ and the restricted Hartree Fock (HF) theory employing a STO-3G and a STO-3-G* basis¹⁶⁾.

In Figure 8 we show the PE spectrum of **4**. The ionization energies of the first bands of the PE spectrum of **4** are collected in Table 7.

In the PE spectrum of **4** we recognize three peaks, two with steep onset at 6.7 and 8.1 eV and a very broad band around 7.5 eV.

Figure 8. He(I) PE spectrum of decamethylsilicocene (**4**)Table 7. Comparison between the first vertical ionization energies, $I_{v,j}$, of **4** with the calculated orbital energies, ϵ_j , of **5**; all values in eV

Band	$I_{v,j}$	Assignment C_5	$-\epsilon_j$ (MNDO) ^{a)}	$-\epsilon_j$ (STO-3G) ^{a)}	$-\epsilon_j$ (STO-3G*) ^{b)}
1	6.7	16a''	8.67	5.83	6.47
		26a'	8.68	5.83	6.53
2	7.5	25a'	8.83	7.12	7.17
		15a''	9.23	7.83	7.89
3	8.1	24a'	9.23	7.84	8.22

^{a)} The calculations were carried out for **5b** with structural parameters from the GED experiment (Table 5). – ^{b)} The calculations were carried out for **5b** with structural parameters optimized at the STO-3G level.

Ionization events from weakly bonding π -MOs usually give rise to steep bands, while Gaussian-like bands are encountered when ionization occurs from bonding MOs or lone pairs. From these empirical arguments we tentatively assign bands 1 and 3 to ionizations from π -MOs, band 2 to the lone pair at silicon.

To compare this empirical result with the outcome of MO calculations we relate the vertical ionization energies, $I_{v,j}$, with the calculated orbital energies, ϵ_j , by assuming the validity of Koopmans' theorem ($-\epsilon_j = I_{v,j}$)¹⁷. This assumption is fairly good for the main-group elements if it is restricted to the outer valence region.

Earlier calculations on the parent silicocene (**5**) using the MNDO method yielded contradictory results. While Cowley et al. reported the bis(pentahapto) structure to be the global minimum¹⁸, Glidewell predicted the bis(monohapto) isomer **5h** to be the most stable isomer¹⁹. The results of our semiempirical and HF SCF calculations are collected in Table 8. For **5g** and **5h** we noticed convergence problems, probably because a one-determinantal description of these structures is not adequate.

Table 8. Relative energies [kcal/mol] for $(\text{H}_5\text{C}_5)_2\text{Si}$ using the MNDO and the HF-SCF method with a STO-3G and STO-3G* basis

Structure Model	ΔE [kcal/mol]			
	MNDO ^{b)}	STO-3G ^{a)}	STO-3G ^{b)}	STO-3G* ^{c)}
5a (D_{5d})	28.0	4.8	17.8	11.6
5b (C_s)	4.3	0	0	0
5c (D_{5h})	28.0	4.8	17.8	11.6
5d (C_{2v})	5.7	0.1	0.7	0.5
5e (C_{2v})	6.2	0.1	2.9	1.4
5f (C_s)	0	53.8	48.1	52.8
5i (C_{2h})	28.0	9.6	17.8	11.6

^{a)} With structural parameters of **4a** and **4b**. — ^{b)} Based on the optimized structures. — ^{c)} With the geometrical parameters optimized at the STO-3G level and augmented basis set by d functions on the central atom ($\alpha_d^{\text{Si}} = 0.39$).

According to the nonempirical results, **5b** is predicted to be the global minimum of the manifold. The energy difference to structures **5d** and **5e** is too small to be of any significance. Since **5b**, **5d**, **5e** are only rotamers with respect to the silicon–cyclopentadienyl bond this result is anticipated. It is interesting to note that the energy for **5i** is predicted to be very close to that derived for **5a** and **5c**, in fact **5i** converges during the minimization process to **5a**. Our results agree with very recent ab initio calculations of **5**²⁰. The results are fully in line with the experiments, i.e., favouring a more or less bent bis(pentahapto) structure with a low energy barrier for the rotation of the cyclopentadienyl rings.

Table 9. Optimized geometrical parameters of **5a**–**5e** as derived by a HF-SCF calculation with STO-3G basis; for the meaning of d , α , Θ , and $\chi_{\text{C}_5\text{C}_5}$ see Table 4 and Figure 5

Parameters	5a (D_{5d})	5b (C_s)	5c (D_{5h})	5d (C_{2v})	5e (C_{2v})
d	2.089	2.151	2.089	2.160	2.121
$r(\text{Si}-\text{C})$ (range)	2.407	2.089–2.804	2.406	2.166–2.787	2.117–2.687
$r(\text{C}1-\text{C}2)$	1.405	1.408	1.405	1.408	1.408
$r(\text{C}-\text{H})$	1.078	1.078	1.078	1.078	1.078
α	—	153.8	—	155.9	155.3
Θ	—	19.6	—	19.8	15.8
$\chi_{\text{C}_5\text{C}_5}$	—	65.4	—	63.7	56.3

A comparison between the calculated geometrical parameters for **5a**–**5e** (see Table 9) with those derived from the GED results yields a fairly good agreement as concerns the distances. As experienced in other cases with a minimal basis set¹⁶ the bond lengths are predicted slightly shorter than found by experiment. Large discrepancies are encountered for the angles describing the bending of the rings. The bending is predicted to be larger in **5b** as compared to **4b**. This is anticipated since the methyl groups in **4** interfere seriously at larger Θ angles.

The MNDO results favour **5f** as the global minimum and predict similar energies for **5b**, **5d**, and **5e** as well as **5a** and **5c** (Table 8). We ascribe the preference of **5f** to the parametrization for Si within the MNDO approach. In this connection it is interesting to note that nonempirical calculations carried out on $(\text{H}_5\text{C}_5)_2\text{P}^{\oplus}$ predict²¹ an $(\eta^1\text{-H}_5\text{C}_5)(\eta^2\text{-H}_5\text{C}_5)\text{P}^{\oplus}$ (C_s) structure to be the minimum.

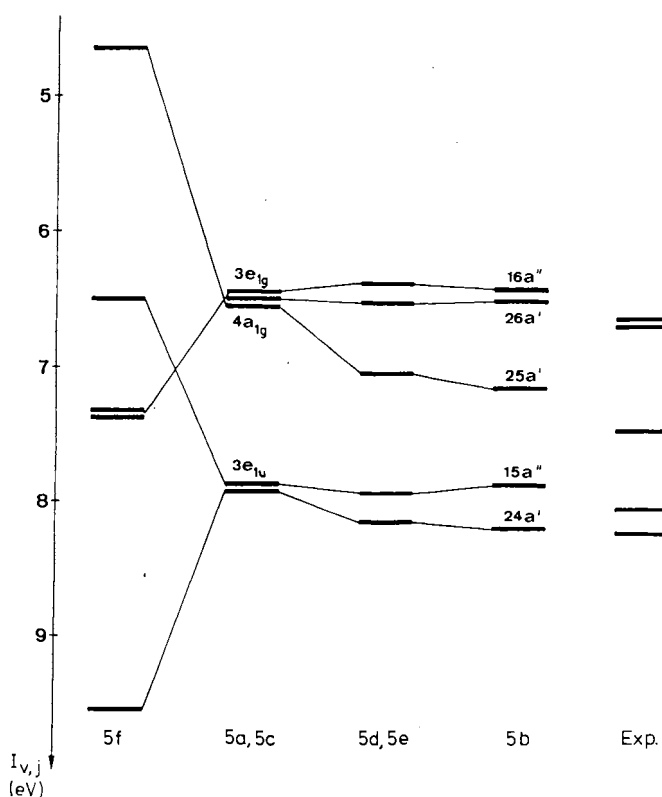


Figure 9. Comparison between the first five calculated orbital energies at the STO-3G* level of **5a**–**5f** with the measured ionization energies assuming Koopmans' theorem

In Table 7 and Figure 9 we have compared the calculated orbital energies for **5** with the measured ionization energies for **4**. We notice a fairly good agreement between the relative splitting found for structures **5b**, **5d**, and **5e** and the experiment. The agreement with respect to the absolute numbers is fortuitous since the calculated orbital energies refer to the parent compound and the experiment to the decamethyl derivative. The HF-SCF calculations with small basis sets usually predict the ionization energies much lower than the experiment. This shortcoming is just balanced by the methyl groups in our example. For the structures **5a** and **5c** the predicted energy difference of the first three orbital energies is too small. The disagreement between the predicted orbital pattern of **5f** and the experiment is evident.

In Figure 10 we have drawn schematically the five highest occupied MOs of **5a**. It is seen that the two highest occupied MOs are localized only on the ligands while $4a_{1g}$ is an antibonding combination between the 3 s atomic orbital on Si and the 2 p_{π} -MOs of the ligands. The MOs $3e_{1u}$ can be described as the bonding linear combinations between 3 p orbitals of silicon and 2 p_{π} -MOs of the ligands.

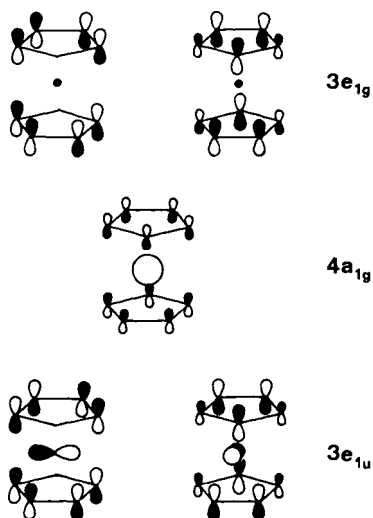


Figure 10. Schematic drawing of the five highest occupied MOs of **5a** (D_{5d})

Further evidence in support of a bis(pentahapto) structure is a similar split between the PE bands of e'_1 and e'_2 of several dicyclopentadienyl compounds with bis(pentahapto) structure like beryllocene (center of gravities: 1.6 eV)²², and decamethylmagnesocene (0.7 eV)²³. If structures **5f**–**5h** were present in the gas phase we expect to observe the π -bands of one or two cyclopentadiene units in the corresponding PE spectrum. The split between these bands which are due to b_2 (π) and a_2 (π) should be in the order of 2 eV as found in the PE spectrum of hexamethylcyclopentadiene²⁴.

For a comparison of the PE data of **4** with decamethylgermanocene (**6**), decamethylstannocene (**7**), and decamethylplumbocene (**8**) we have remeasured the PE spectrum of **8**, because Cowley et al. reported a very low ionization energy for the first PE band (6.33 eV)¹⁸. In Figure 11 the PE spectrum of **8** is depicted. We ascribe the first peak at 6.3 eV to an impurity, the reason being its low intensity as compared to the other bands and the dependency on the intensity of this band on the recording conditions.

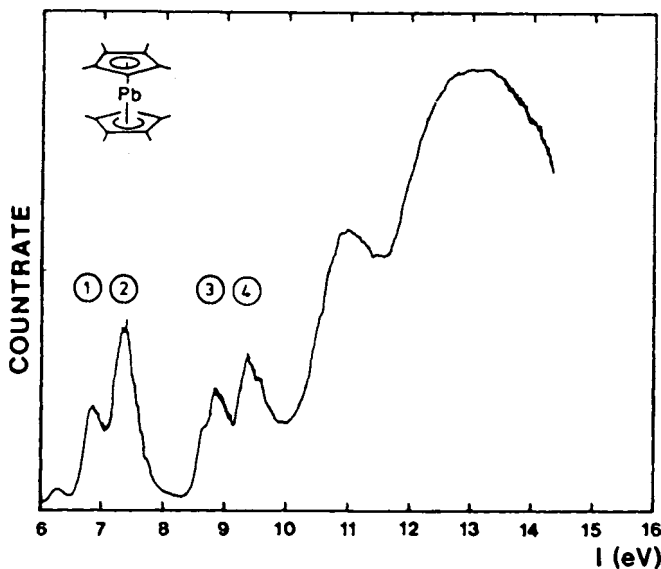


Figure 11. He(I)-PE spectrum of decamethylplumbocene (**8**)

In Figure 12 we have compared the first PE bands of **4** with those of its congeners **6**²⁵ and **7**²⁵. A comparison between these three PE spectra shows a strong shift to higher energy of the band assigned to the group 14 element lone pair and a slight decrease of the energy difference between the ligand bands in going from **7** to **6** and **4**. We ascribe both shifts to the stronger overlap between silicon and carbon compared to germanium, tin, and carbon, respectively. The stronger overlap makes the interaction in $4a_{1g}$ more antibonding and strengthens the bonding in $3e_{1u}$ (see Figure 10). As a result we expect a destabilization of $4a_{1g}$ and a stabilization of $3e_{1u}$ in the case of the silicon with respect to the germanium and the tin compound. The PE data available from decamethylplumbocene allow no unequivocal assignment of the PE bands, therefore we have not included them in Figure 12.

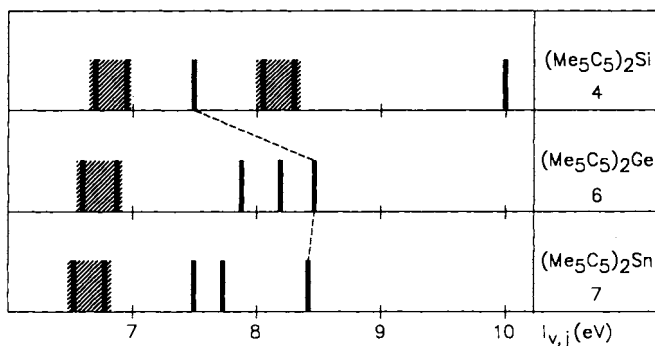


Figure 12. Comparison between the first bands in the PE spectra of **4**, **6**, and **7**

The electronic absorption spectra of **4** and **6**–**8** show a bathochromic shift³¹ (**4**: colorless, **6**: light yellow, **7**: orange, and **8**: red). If we use a one-electron model to rationalize this observation we come to the conclusion that the LUMO in the above series should be lowered, because the HOMO

($3e_{1g}$) remains essentially constant (see Figure 12). This assumption is corroborated by the result of a MNDO calculation on the parent compounds which shows a HOMO/LUMO gap of 8.16 eV for **5**, 7.97 eV for $(H_5C_5)_2Ge$, and 7.15 eV for $(H_5C_5)_2Sn$. The LUMO ($4e_{1u}$) can be described as the antibonding linear combination between the ligand π -MOs and p_x and p_z , respectively, at the central atom. Thus the lowering in energy of $4e_{1u}$ within the series $(H_5C_5)_2Si$, $(H_5C_5)_2Ge$, and $(H_5C_5)_2Sn$ can be traced back to a decrease in the overlap integrals between the p orbitals of the central atoms and the π -MOs of the cyclopentadienyl ligands. The antibonding character of $4e_{1u}$ is reduced in this series.

We are grateful to the *Deutsche Forschungsgemeinschaft* and to the *Fonds der Chemischen Industrie* for financial support. We thank Prof. W. W. Schoeller and Dipl.-Chem. I. Niemann for the CV measurements and for helpful discussions.

Experimental

All manipulations were carried out under N_2 or Ar by using standard Schlenk techniques. Solvents were distilled from drying agents and degassed three times prior to use. — NMR studies: Bruker AM 300 spectrometer; 1H NMR (300 MHz, TMS ext.), ^{13}C NMR (75 MHz, TMS ext.), ^{29}Si NMR (59 MHz, TMS ext.); chemical shifts in ppm. — Elemental analyses: Microanalytical Laboratory of the Faculty of Chemistry, University of Bielefeld; Microanalytical Laboratory Beller, Göttingen. — Melting point determination: Büchi 510 (capillary melting point apparatus). — Mass spectra: Varian 311 A. — CV studies: PAR 173 potentiostat-galvanostat with integrated PAR 179 digital coulometer and PAR 175 universal programmer. — He(I) PE spectra: Perkin-Elmer PS 18; calibration with Ar and Xe. — Space-filling models: SCHAKAL program. — X-ray crystallographic studies: Nonius CAD 4 diffractometer, further details see Table 1. — GED studies: Gas-phase electron diffraction patterns have been recorded on a Balzers El-diograph KD-G2 with an accelerating potential of 42 kV. The electron wavelength was calibrated against diffraction patterns of benzene [$r(C-C) = 139.75$ pm], with an estimated uncertainty of 0.1%. A conventional nozzle was used with nozzle and reservoir temperatures of 242(8)°C. The rubber o-rings were substituted with teflon o-rings because of the high temperatures. No sign of decomposition was observed. Exposures were made with nozzle-to-plate distances of 498.43 and 248.00 mm. The plates were subjected to photometry and the optical densities processed by standard procedures²⁸⁾. Four plates were used from each camera distance with s ranging from 15.0 to 150.0 nm⁻¹ with $\Delta s = 1.25$ nm⁻¹ (long camera distance), and with s ranging from 50.0 to 300.0 nm⁻¹ with $\Delta s = 2.5$ nm⁻¹ (short). The backgrounds were computer-drawn by a least-squares fit of the sum of a polynomial and a theoretical molecular intensity curve to the experimental levelled intensity curves. The degree of the polynomial was 8 for all curves. Least-squares refinements of the structural parameters were performed on an average curve for each camera distance. Complex atomic scattering factors, $f'(s)$, were calculated from an analytical representation of the atomic Hartree-Fock-Slater potentials for Si and C²⁹⁾ and from a bonded potential for H³⁰⁾.

Decamethylsilicocene (**4**)

a) According to Eq. 2: To a solution of 30.80 g (83.4 mmol) of **2** in 600 ml of 1,2-dimethoxyethane, a solution of 250 mmol of naphthalene-sodium [prepared from 5.75 g (250 mmol) of sodium and 32.04 g (250 mmol) of naphthalene] in 200 ml of 1,2-dimethoxyethane is added during 3 h at -55°C. After stirring at room temp.

for 12 h and evaporation of the solvent, the brownish residue is extracted with 600 ml of *n*-pentane. Evaporation of the solvent and fractional sublimation yields 12.30 g (49%) of **4**. — M. p. 169°C. — 1H NMR (C_6D_6): $\delta = 1.89$. — ^{13}C NMR (C_6D_6): $\delta = 10.3$ [Me_3C_5], 119.2 [Me_3C_5]. — ^{29}Si NMR (C_6D_6): $\delta = -392.0$. — MS (70 eV): m/z (%) = 163 (100) [$M^+ - C_5Me_5$].

$C_{20}H_{30}Si$ (298.5) Calcd. C 80.46 H 10.13

Found C 80.35 H 10.11

Mol. mass 290 (cryoscopically in benzene)

b) According to Eq. 3: To a solution of 0.51 g (1.11 mmol) of **3** in 20 ml of THF, a solution of 2.20 mmol of anthracene-potassium in 10 ml of THF is added at -20°C. Workup in analogy to procedure a) finally leads to 0.31 g (95%) of **4**.

Reaction of **4** with Naphthalene-Sodium according to Eq. 4: To a solution of 1.18 g (3.85 mmol) of **4** in 25 ml THF, a solution of 7.90 mmol of naphthalene-sodium [prepared from 181.6 mg (7.90 mmol) of sodium and 1.20 g (9.35 mmol) of naphthalene] in 40 ml of THF is added at -78°C. After stirring at room temp. for 12 h and evaporation of the solvent, the brownish residue is extracted with 50 ml of *n*-pentane. According to 1H -NMR data, the *n*-pentane solution only contains naphthalene [$\delta = 7.21-7.27$ (m, 4H), 7.59-7.64 (m, 4H)]. After addition of ethanol to the residue, the presence of pentamethylcyclopentadiene in the solution is proved by 1H -NMR spectroscopy [$\delta = 1.01$ (d, $J = 7.8$ Hz, 3H), 1.69 (br. s, 12H), 2.48 (q, $J = 7.8$ Hz, 1H)].

CAS Registry Numbers

2: 100189-22-8 / **3**: 113475-40-4 / **4**: 100189-23-9 / $NaC_{10}H_8$: 3481-12-7 / $KC_{10}H_{14}$: 34475-54-2 / $LiC_{10}H_8$: 120637-49-2 / $KC_{10}H_8$: 4216-48-2 / $(H_5C_5)_2Si$: 81790-05-8 / $(Me_3C_5)_2Pb$: 120637-50-5 / pentamethylcyclopentadiene: 4045-44-7

- ¹⁾ P. Jutzi, *Adv. Organomet. Chem.* **26** (1986) 217.
- ²⁾ Y.-N. Tang, *Reactions of Silicon Atoms and Silylenes* (R. A. Abramovitch, Ed.), *Reactive Intermediates*, vol. 2, ch. 4, p. 297-366, Plenum, New York 1982.
- ³⁾ P. P. Gaspar, *Silylenes* (M. Jones, Jr., R. A. Moss, Eds.), *Reactive Intermediates*, vol. 3, p. 335-385, Wiley, New York, 1985.
- ⁴⁾ P. Jutzi, D. Kanne, M. B. Hursthouse, A. J. Howes, *Chem. Ber.* **121** (1988) 1299.
- ⁵⁾ P. Jutzi, B. Hielscher, *Organometallics* **5** (1986) 1201.
- ⁶⁾ P. Jutzi, *Comments on Inorg. Chem.* **6** (1987) 123.
- ⁷⁾ P. Jutzi, D. Kanne, C. Krüger, *Angew. Chem.* **98** (1986) 163.
- ⁸⁾ G. R. Stevenson, I. Valentin, E. Williams Jr., G. Caldwell, A. E. Alegria, *J. Am. Chem. Soc.* **101** (1975) 515.
- ⁹⁾ P. Jutzi, R. Dickbreder, H. Nöth, *Chem. Ber.* **122** (1989) 865.
- ¹⁰⁾ A. G. Davies, I. Luszyk, *J. Chem. Soc., Chem. Commun.* **1980**, 554; *J. Chem. Soc., Perkin Trans. 2*, **1981**, 692.
- ¹¹⁾ P. Jutzi, D. Kanne, U. Holtmann, W. W. Schoeller, unpublished results.
- ¹²⁾ R. A. Anderson, R. Blom, J. M. Boncella, C. J. Burns, H. V. Volden, *Acta Chem. Scand., Ser. A*, **41** (1987) 24.
- ¹³⁾ R. Bloom, A. Haaland, unpublished results.
- ¹⁴⁾ L. Fernholt, A. Haaland, P. Jutzi, F. X. Kohl, R. Seip, *Acta. Chem. Scand., Ser. A*, **38** (1984) 121.
- ¹⁵⁾ M. J. S. Dewar, W. Thiel, *J. Am. Chem. Soc.* **99** (1977) 4899; M. J. S. Dewar, M. L. KcKee, H. S. Rzepa, *ibid.*, **100** (1978) 3607.
- ¹⁶⁾ W. J. Hehre, L. Radom, P. v. R. Schleyer, J. A. Pople, *ab initio Molecular Orbital Theory*, J. Wiley & Sons, New York 1986.
- ¹⁷⁾ T. Koopmans, *Physica I* (1934) 104.
- ¹⁸⁾ S. G. Baxter, A. H. Cowley, J. G. Lasch, M. Lattman, W. P. Sharum, C. A. Stewart, *J. Am. Chem. Soc.* **104** (1987) 4064.
- ¹⁹⁾ C. Glidewell, *J. Organomet. Chem.* **286** (1985) 289.
- ²⁰⁾ M. S. Gorden, K. K. Baldrige, J. A. Bock, S. Kosecki, M. W. Schmidt in *Silicon Chemistry* (J. Y. Corey, E. R. Corey, P. P. Gaspar, Eds.), p. 459, Ellis Horwood Ltd., Chichester 1987; T. J. Lee, J. E. Rice, *J. Am. Chem. Soc.* **111** (1989) 2011.

- ²¹ T. J. Lee, H. F. Schaefer III, E. A. Magnusson, *J. Am. Chem. Soc.* **107** (1985) 7239.
- ²² R. Gleiter, M. C. Böhm, A. Haaland, R. Johanson, J. Lusztyk, *J. Am. Chem. Soc.* **107** (1979) 285.
- ²³ C. Cauletti, J. C. Green, M. R. Kelly, P. Powell, J. VanTilborg, J. Robbins, J. Smart, *J. Electron. Spectrosc. Rel. Phen.* **19** (1980) 327.
- ²⁴ R. Gleiter, P. Jutzi, unpublished results.
- ²⁵ G. Bruno, E. Ciliberto, I. L. Fragala, P. Jutzi, *J. Organomet. Chem.* **289** (1985) 268.
- ²⁶ P. Jutzi, F. Kohl, P. Hofmann, C. Krüger, Y. H. Tsay, *Chem. Ber.* **113** (1980) 757.
- ²⁷ I. L. Atwood, W. E. Hunter, A. H. Cowley, R. A. Iones, C. A. Stewart, *J. Chem. Soc., Chem. Commun.* **1981**, 925.
- ²⁸ B. Andersen, H. M. Seip, T. G. Strand, R. Stolevik, *Acta Chem. Scand.* **23** (1969) 3224.
- ²⁹ T. G. Strand, R. A. Bonham, *J. Chem. Phys.* **40** (1964) 1686; A. C. Yates, *Comput. Phys. Commun.* **2** (1971) 175.
- ³⁰ R. F. Stewart, E. R. Davidson, W. T. Simpson, *J. Chem. Phys.* **42** (1965) 3175.
- ³¹ Precise measurements are not possible due to decomposition of the metallocenes in dilute solution.

[90/89]